Journal of Peptide Science
J. Pept. Sci. 2008; **14**: 1259–1270
Published online 24 September 2008 in Wiley InterScience (www.interscience.wiley.com). DOI: 10.1002/psc.1066

JOURNAL OF PEPTIDE SCIENCE

Computational studies on the backbone-dependent side-chain orientation induced by the (*S,S*)-CXC motif

ATHANASSIOS STAVRAKOUDIS[a,b]* and VASSILIOS TSIKARIS[b]

[a] Department of Economics, University of Ioannina, GR-451 10 Ioannina, Greece
[b] Department of Chemistry, University of Ioannina, GR-451 10 Ioannina, Greece

Received 13 March 2008; Revised 19 June 2008; Accepted 6 July 2008

Abstract: Disulfide cyclization is a well-known procedure to impose conformational restriction to peptides undergoing backbone flexibility. Rigid conformations are induced only for small rings with a specific combination of amino acids. In this work, we present a computational search of the backbone and backbone-dependent side-chain orientation of two series of linear and cyclic peptide analogs. The -C[XY]C- scaffold (where X,Y is arginine, aspartic acid or alanine residue) in its open and (S,S) cyclic form was used for the design of the studied analogs. Thirty-six compounds, resulting from the extension with one residue at either the *N*- or the *C*-terminus were studied with classical MD. The local backbone conformation and the relative orientation of the X and Y side chains induced by either cyclization and/or the presence of the charged residues are discussed. From the present study it is concluded that cyclization has a great impact on the *synplanar* orientation of the X and Y side chains in the (S,S)Ac-XCYC-NH_2 series of compounds while charge–charge interaction has only a weak synergic effect. On the contrary, the *antiplanar* orientation is favored in the case of (S,S)Ac-CXCY-NH_2. Copyright © 2008 European Peptide Society and John Wiley & Sons, Ltd.

Keywords: computational alanine scanning; backbone-dependent orientation; charge–charge interaction; computer simulation; cyclic peptides; disulfide cyclization; molecular dynamics; side-chain conformation

INTRODUCTION

Development of peptide-based drugs requires the evaluation of structure-activity relationships, which is facilitated by incorporation of conformational constraints. Peptidomimetics or other specific modifications limit the number of conformations of otherwise flexible peptides [1]. A significant amount of effort has been focused on the design and synthesis of small molecules for stabilizing specific backbone peptide conformations. Various bioactive compounds have been synthesized incorporating nonpeptide residues especially β-turn mimetics [2]. One of the most often utilized approaches to introduce conformational constraints is cyclization [3]. Disulfide cystine linkages have a great effect on the conformational freedom of protein molecules [4,5]. There are many examples of using disulfide linkages to introduce conformational constraints such as β-turns and β-sheets. A number of studies have mainly focused on the propensity of the cyclic tetrapeptides, containing the -CXYC- motif, to form β-turns or α-helices [6,7]. This sequence, the smallest and most highly conserved chelating unit in biological systems, is known to be an essential motif at active-sites of disulfide oxidoreductases for their catalysis of redox reactions [6]. Owing to this biological significance of the -CXYC- sequence, many experimental and theoretical studies have been reported aiming to evaluate factors that influence its backbone conformational preferences. However, in most cases side-chain orientations represent the key factor for an optimum recognition event. In a typical protein–ligand system the orientation of side chains can have considerable consequences. For example, the hydroxyl group of a tyrosine side chain is moving 9 Å when the orientation changes from g^- to t conformation [8]. The significance of side-chain conformations imposed the development of various rotamer libraries used in protein structure prediction, protein design and structure refinement [8–11]. However, up to now little research has been done on peptide scaffolds with backbone constraints that could restrict side-chain flexibility and induce specific orientations. Such scaffolds can be very useful for the design and development of bioactive compounds. A notable example of (S,S)-CXC- motif is the Tyr-c[D-Cys-Phe-D-Pen]OH peptide (JOM13) which has been used as a delta-opioid farmacophore [12–15].

In previous studies we reported on a new class of cyclic (S,S) non-RGD containing peptide sequences, utilizing two cysteine residues as a structural scaffold for the development of promising antiaggregatory agents with biomedical potential [16]. These compounds were found to be very potent inhibitors of the human platelet aggregation ($IC_{50} \sim 1–10$ μM). The IC_{50} values are 10–20 times lower in inhibiting the fibrinogen binding to activated human platelets [16]. The (S,S)-CDC- sequence was incorporated, as a conformational constraint, in molecules bearing at least one positive charge with the general formula (S,S)XCDCZ, where X and Z are various amino acids [17]. Conformational

*Correspondence to: Athanassios Stavrakoudis, Department of Economics, University of Ioannina, GR-45110 Ioannina, Greece;
e-mail: astavrak@cc.uoi.gr

searching by molecular modeling calculations revealed that incorporation of (*S*,*S*)-CDC- motif favors the orientation of the charged side chains toward the same side of the molecule. The dihedral angle (*pdo*) formed by the Arg:C^{ζ}, Arg:C^{α}, Asp:C^{α} and Asp:C^{γ} atoms was selected to define the Arg and Asp side-chain orientation. The fulfillment of the criterion: $-45^{\circ} \leq pdo \leq +45^{\circ}$, was shown to be correlated with the antiaggregatory activity of these analogs [16,18,19]. The above-mentioned studies revealed that constraints for inducing specific orientations of the side chains are of great importance for the development of peptide-based bioactive compounds of medicinal interest.

In this study, we performed an extensive conformational searching of the peptide sequences Ac-XCYC-NH_2, (*S*,*S*) Ac-XCYC-NH_2, Ac-CXCY-NH_2, and (*S*,*S*) Ac-CXCY-NH_2, where X,Y can be alanine, arginine or aspartic residue (Table 1), using MD techniques [20,21]. These amino acids were selected in order to evaluate the factors, such as cyclization, charge–charge interactions, and sequence that influence the relative orientation of the side chains of the X and Y amino acids.

EXPERIMENTAL METHODS

All simulations were performed using the TINKER package [22] (version 4.1) on a LINUX machine. The simulation protocol was very similar as in Ref. 16. The AMBER94 parameter set [23] was used in all molecular mechanics (MM) and MD calculations. Peptide analogs were initially built in fully extended conformation, with all dihedral angles set to 180°. Each peptide was energy minimized with 300 steps of L-BFGS and the resulting conformation was subjected to MD at 300 K, for 2.2 ns. The Verlet algorithm was used for numerical integration of motion with time, a step of 1 fs. In both MM and MD runs, the solvent accessible surface area (SASA) model of macroscopic representation of the solvent [24–26] was used with a dielectric constant of 4. A dual cutoff was applied for non-bonded interactions, 15 and 12 Å for electrostatic and van der Waals interactions respectively. During the MD runs a snapshot was saved every 1 ps, resulting in 2200 frames in each trajectory. The last 2000 frames were used for analysis presented here. Visualization and graphics were performed with visual molecular dynamics (VMD) [27] and PyMol [28].

Conformational states of each residue in the resulting trajectories were classified according to Zimmerman (Figure 1), who described a conformational state by a one-letter code [29]. Each trajectory was clustered according to a three-letter code describing the conformational state of the -XCY- sequence either in the Ac-XCYC-NH_2 or in the Ac-CXCY-NH_2 analogs. Clusters with less than 10% population were excluded from the analysis presented in this work. Secondary structure assignments were computed with the STRIDE [30] program. Statistical analyses of the angular data were computed taking into consideration the von Mises distribution (circular normal distribution).

In addition to *pdo*, the dihedral angle pdo_{β}, defined by Cβ(X)-Cα(X)-Cα(Y)-Cβ(Y) atoms in the -XCY- sequence, was also used as a measure of the X,Y side-chain orientation. The X, Y side-chain proximity was evaluated by measuring the distance ($d_{\beta\beta}$) between Cβ(X) and Cβ(Y). The distance ($d_{\zeta\gamma}$) between Cζ(R) and Cγ(D) was used as a measure of the charge–charge side-chain interaction.

Home-made scripts (Bash, Perl, SQL and R) used for analysis are available upon request.

Table 1 Linear and cyclic peptides studied with molecular dynamics simulations

No	Peptide (linear)	Sequence	No	Peptide (cyclic)	Sequence
1	ACAC	Ac^1-Ala^2-Cys^3-Ala^4-Cys^5-NH_2	2	cACAC	(*S*, *S*)Ac^1-Ala^2-Cys^3-Ala^4-Cys^5-NH_2
3	RCAC	Ac^1-Arg^2-Cys^3-Ala^4-Cys^5-NH_2	4	cRCAC	(*S*, *S*)Ac^1-Arg^2-Cys^3-Ala^4-Cys^5-NH_2
5	ACRC	Ac^1-Ala^2-Cys^3-Arg^4-Cys^5-NH_2	6	cACRC	(*S*, *S*)Ac^1-Ala^2-Cys^3-Arg^4-Cys^5-NH_2
7	DCAC	Ac^1-Asp^2-Cys^3-Ala^4-Cys^5-NH_2	8	cDCAC	(*S*, *S*)Ac^1-Asp^2-Cys^3-Ala^4-Cys^5-NH_2
9	ACDC	Ac^1-Ala^2-Cys^3-Asp^4-Cys^5-NH_2	10	cACDC	(*S*, *S*)Ac^1-Ala^2-Cys^3-Asp^4-Cys^5-NH_2
11	RCDC	Ac^1-Arg^2-Cys^3-Asp^4-Cys^5-NH_2	12	cRCDC	(*S*, *S*)Ac^1-Arg^2-Cys^3-Asp^4-Cys^5-NH_2
13	DCRC	Ac^1-Asp^2-Cys^3-Arg^4-Cys^5-NH_2	14	cDCRC	(*S*, *S*)Ac^1-Asp^2-Cys^3-Arg^4-Cys^5-NH_2
15	DCDC	Ac^1-Asp^2-Cys^3-Asp^4-Cys^5-NH_2	16	cDCDC	(*S*, *S*)Ac^1-Asp^2-Cys^3-Asp^4-Cys^5-NH_2
17	RCRC	Ac^1-Arg^2-Cys^3-Arg^4-Cys^5-NH_2	18	cRCRC	(*S*, *S*)Ac^1-Arg^2-Cys^3-Arg^4-Cys^5-NH_2
19	CACA	Ac^1-Cys^2-Ala^3-Cys^4-Ala^5-NH_2	20	cCACA	(*S*, *S*)Ac^1-Cys^2-Ala^3-Cys^4-Ala^5-NH_2
21	CRCA	Ac^1-Cys^2-Arg^3-Cys^4-Ala^5-NH_2	22	cCRCA	(*S*, *S*)Ac^1-Cys^2-Arg^3-Cys^4-Ala^5-NH_2
23	CACR	Ac^1-Cys^2-Ala^3-Cys^4-Arg^5-NH_2	24	cCACR	(*S*, *S*)Ac^1-Cys^2-Ala^3-Cys^4-Arg^5-NH_2
25	CDCA	Ac^1-Cys^2-Asp^3-Cys^4-Ala^5-NH_2	26	cCDCA	(*S*, *S*)Ac^1-Cys^2-Asp^3-Cys^4-Ala^5-NH_2
27	CACD	Ac^1-Cys^2-Ala^3-Cys^4-Asp^5-NH_2	28	cCACD	(*S*, *S*)Ac^1-Cys^2-Ala^3-Cys^4-Asp^5-NH_2
29	CDCR	Ac^1-Cys^2-Asp^3-Cys^4-Arg^5-NH_2	30	cCDCR	(*S*, *S*)Ac^1-Cys^2-Asp^3-Cys^4-Arg^5-NH_2
31	CRCD	Ac^1-Cys^2-Arg^3-Cys^4-Asp^5-NH_2	32	cCRCD	(*S*, *S*)Ac^1-Cys^2-Arg^3-Cys^4-Asp^5-NH_2
33	CDCD	Ac^1-Cys^2-Asp^3-Cys^4-Asp^5-NH_2	34	cCDCD	(*S*, *S*)Ac^1-Cys^2-Asp^3-Cys^4-Asp^5-NH_2
35	CRCR	Ac^1-Cys^2-Arg^3-Cys^4-Arg^5-NH_2	36	cCRCR	(*S*, *S*)Ac^1-Cys^2-Arg^3-Cys^4-Arg^5-NH_2

DOI: 10.1002/psc

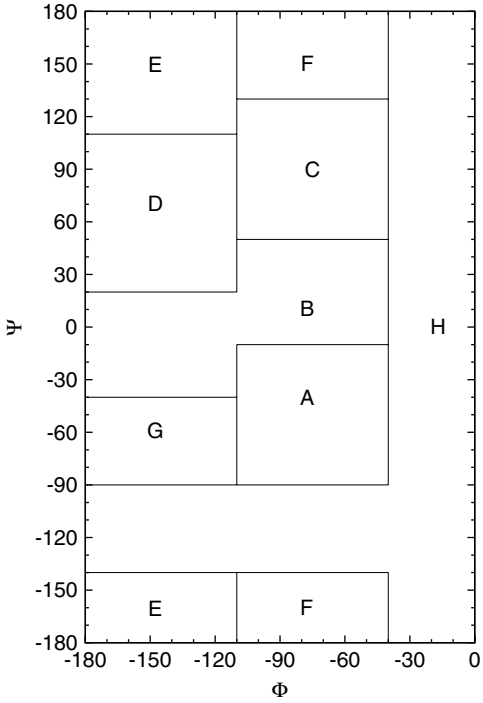

Figure 1 Conformational states according to Zimmerman (see text for details).

RESULTS AND DISCUSSION

All simulations gave stable MD trajectories (each of them took approximately 48 CPU hours). For simplicity we divide the presentation of the results in two parts: the Ac-XCYC-NH_2 and the Ac-CXCY-NH_2 motifs. In the present analysis, the *synplanar* and *antiplanar* orientations of the X and Y side chains were arbitrarily accepted, if the pdo_β values were found within the regions of $|pdo_\beta| < 45^\circ$ and $|pdo_\beta| > 135^\circ$ respectively. Table 2 summarizes the percentage of the frames in which the X and Y side chains adopt the *synplanar* and *antiplanar* orientations.

The Ac-X^2CY^4C-NH_2 Class of Analogs

Ac-A^2CAC^5-NH_2, (S,S)Ac-A^2CAC^5-NH_2. As is shown in Table 3, all three residues (-CAC-) of the linear Ac-ACAC-NH_2 adopt either A or B states. The pdo_β angle values fall within the region (120°, −150°) indicating an antiplanar orientation of the two alanine side chains (Table 2, Figure 2). Interestingly the distribution of pdo_β and $d_{\beta\beta}$ is relatively narrow for this short linear peptide (Figure 2). Cyclization induces a transition from A, B to C, D, E and from A, B to C conformational states of Cys^3 and Ala^4 respectively. From Table 3 it is evident that there is no cluster of the -ACA- sequence with the same backbone conformation in linear and cyclic analogs. It seems that cyclization slightly moves towards a more *synplanar* orientation of the X and Y side chains (Figure 2). The percentage of the $|pdo_\beta| < 45^\circ$ values was increased from ~8% in the linear analog to ~14% in the cyclic, while the percentage of the $|pdo_\beta| > 135^\circ$ values was decreased from ~60 to ~41% (Table 2). The above results indicate that cyclization favors the transition from the *antiplanar* to *synplanar* orientation of the A^2 and A^4 side chains in the (S,S)Ac–ACAC–NH_2 peptide.

Table 2 Percentage of frames of each peptide's trajectory, with $|pdo_\beta| < 45^\circ$ values (*synplanar* conformation) and $|pdo_\beta| > 135^\circ$ (*antiplanar* conformation)

No	Peptide (linear)	$\|pdo_\beta\| < 45^\circ$	$\|pdo_\beta\| > 135^\circ$	No	Peptide (cyclic)	$\|pdo_\beta\| < 45^\circ$	$\|pdo_\beta\| > 135^\circ$
1	ACAC	8.2	60.2	2	cACAC	13.7	40.7
3	RCAC	2.9	55.5	4	cRCAC	25.4	19.3
5	ACRC	2.1	72.1	6	cACRC	16.6	27.8
7	DCAC	15.3	36.7	8	cDCAC	9.5	51.3
9	ACDC	27.3	16.3	10	cACDC	33.3	40.4
11	RCDC	0.2	41.2	12	cRCDC	80.1	3.9
13	DCRC	0.2	64.0	14	cDCRC	6.6	11.0
15	DCDC	3.2	20.5	16	cDCDC	42.6	35.6
17	RCRC	0.3	63.7	18	cRCRC	9.7	50.8
19	CACA	3.6	45.8	20	cCACA	1.9	72.1
21	CRCA	6.1	45.7	22	cCRCA	20.6	46.4
23	CACR	1.1	59.1	24	cCACR	1.8	71.9
25	CDCA	0.5	53.9	26	cCDCA	0.1	83.4
27	CACD	22.0	20.5	28	cCACD	2.8	74.9
29	CDCR	0.3	55.8	30	cCDCR	5.2	57.9
31	CRCD	19.5	1.4	32	cCRCD	56.7	1.1
33	CDCD	3.6	44.6	34	cCDCD	18.1	15.5
35	CRCR	3.8	44.8	36	cCRCR	1.0	80.2

DOI: 10.1002/psc

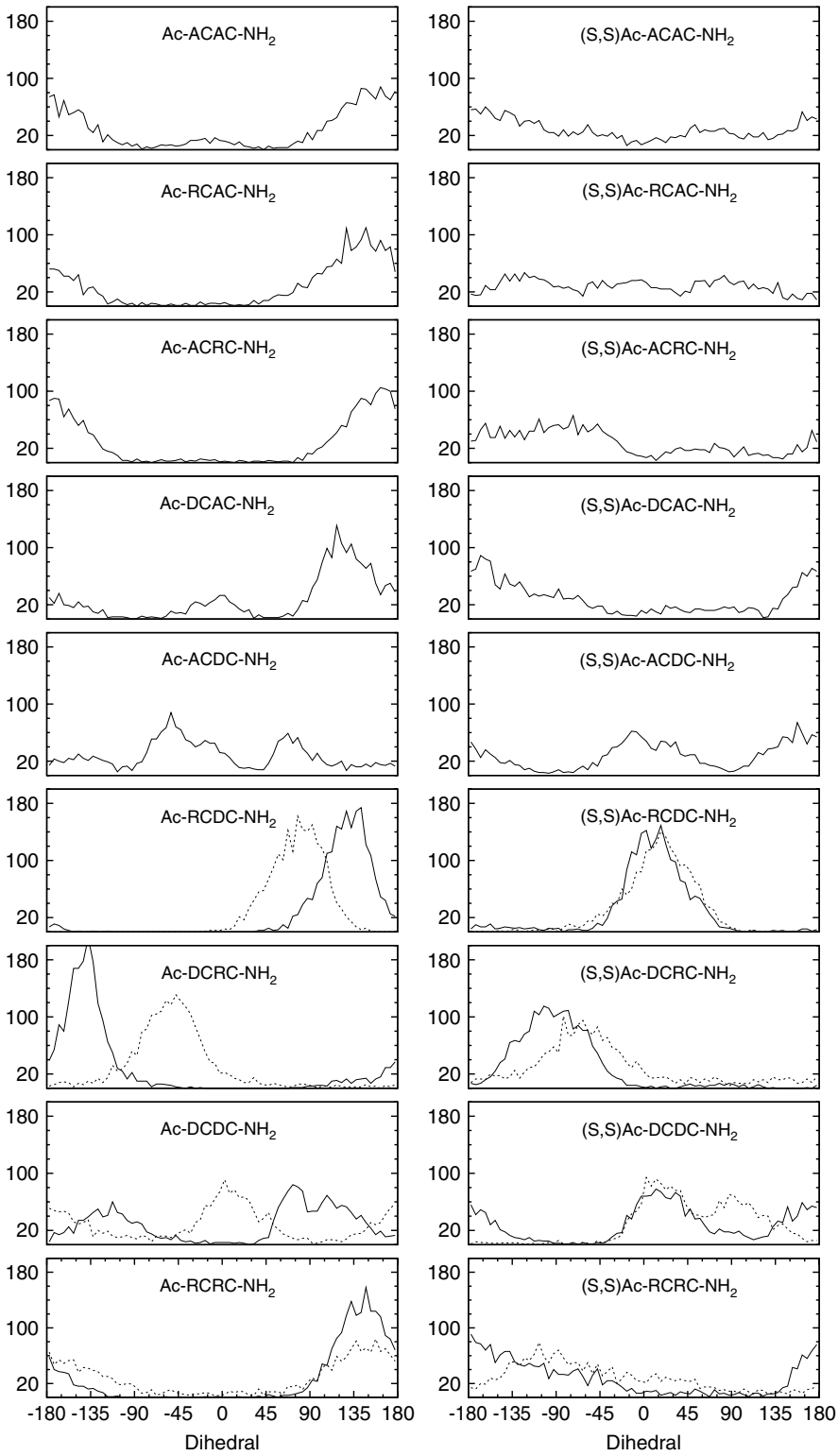

Figure 2 Vertical axis shows number of frames. pdo_{β} (lines) and *pdo* (dashed lines) distribution of the linear and cyclic analogs in the Ac-XCYC-NH_2 series.

Ball and stick representations of the structures are shown in Figure 3.

Ac-R^2CAC^5-NH_2, (S,S)Ac-R^2CAC^5-NH_2. Replacement of A^2 with R^2 residue in the Ac-R^2CAC^5-NH_2 and (*S*, *S*)Ac-R^2CAC^5-NH_2 analogs does not considerably influence either the backbone conformation of the peptide or the distribution of the pdo_{β} angle (Table 2, Figure 2). The conformational states of the individual residues and clusters of the backbone are almost identical to the Ac-A^2CAC^5-NH_2 and (*S*, *S*)Ac-A^2CAC^5-NH_2

DOI: 10.1002/psc

analogs. The previous observation concerning the *synplanar* or *antiplanar* orientation of the R^2 and A^4 side chains is further supported in this case. Thus, the *synplanar* orientation was increased from ~3 to ~25% and the *antiplanar* one was decreased from ~56 to ~19% upon disulfide cyclization (Table 2).

Ac-A²CRC⁵-NH₂, (S,S)Ac-A²CRC⁵-NH₂. When the alanine residue between the two cysteines was replaced by arginine the pdo_β pattern distribution did not change (Figure 2). The pdo_β adopted values close to ±180° in the case of Ac-A^2CRC^5-NH_2. Upon cyclization the *synplanar* orientation of the side chains was favored (the percentage of the *synplanar* orientation was increased from ~2 to 17%, while the *antiplanar* one was decreased from ~72 to ~28%) (Table 2). The conformational similarity of Ac-A^2CAC^5-NH_2 and (S,S)Ac-A^2CAC^5-NH_2 with Ac-A^2CRC^5-NH_2 and (*S*, *S*)Ac-A^2CRC^5-NH_2 respectively is evident if we also compare the conformational states of -A^2CA^4- and -A^2CR^4-sequences (Table 3). In

Table 3 Backbone conformational state, according to Zimmerman classification, of the -XCY- sequence in the Ac-XCYC-NH_2 and Ac-CXCY-NH_2 linear and cyclic peptide series in the clusters with population higher than 10%

No	Peptide (linear)	Zimmerman state cluster	No	Peptide (cyclic)	Zimmerman state cluster
1	ACAC	ABB (10.8) AAA (10.3) ABA (10.1)	2	cACAC	EBB (11.1)
3	RCAC	ABD (10.2)	4	cRCAC	EBB (16.5) EBA (11.6) FBB (11.5) FBA (11.2)
5	ACRC	—	6	cACRC	CCE (27.2) CCB (19.8) DCE (10.1)
7	DCAC	—	8	cDCAC	CCB (21.4) DCB (20.9)
9	ACDC	AAB (17.3) AAA (13.8)	10	cACDC	DCB (41.2) ECB (21.1)
11	RCDC	FAE (12.5) FAF (10.8) FAC (10.8) EAC (10.6)	12	cRCDC	DCB (34.9) ECB (19.7)
13	DCRC	BAA (12.1) AAA (10.2)	14	cDCRC	CCB (46.2) CCE (21.1) CCD (12.2)
15	DCDC	ABA (21.2) AEA (19.2) AAA (17.9)	16	cDCDC	ADC (22.4) FDC (19.4) CDC (13.4)
17	RCRC	AAB (26.6) ABB (21.9) AAA (13.2)	18	cRCRC	ACC (21.9) ADC (17.8) AEC (10.8) BCC (10.7)
19	CACA	ABA (14.6) ABB (14.5) BBA (10.2)	20	cCACA	BBA (13.2) BBB (11.8)
21	CRCA	BAE (15.9)	22	cCRCA	
23	CACR	ABB (18.8) ABA (15.2)	24	cCACR	BBA (17.0) ABA (14.7) BBB (12.7) ABB (10.0)
25	CDCA	ABA (25.1) ABB (22.8) AAA (19.3) AAB (12.3)	26	cCDCA	ABA (20.9) ABB (20.1) BBA (12.4) BBB (11.4) AAA (10.0)
27	CACD	—	28	cCACD	BBB (15.1) BBA (11.9)

DOI: 10.1002/psc

Table 3 (*Continued*)

No	Peptide (linear)	Zimmerman state cluster	No	Peptide (cyclic)	Zimmerman state cluster
29	CDCR	ABB (22.9) ABA (22.0) AAA (14.7)	30	cCDCR	ABA (29.8) ABB (17.8) BBA (15.1) BBB (10.8)
31	CRCD	AAA (12.7) BAB (11.7) BAA (11.1)	32	cCRCD	CEF (36.5) CDF (16.6) CBF (14.9)
33	CDCD	AAB (19.2)	34	cCDCD	DCB (36.8) DCE (4.0) ECB (14.20)
35	CRCR	AAB (23.95) AAA (14.45) BAB (10.95)	36	cCRCR	FBB (25.8) FBA (17.4) FAB (12.4) EBB (11.7)

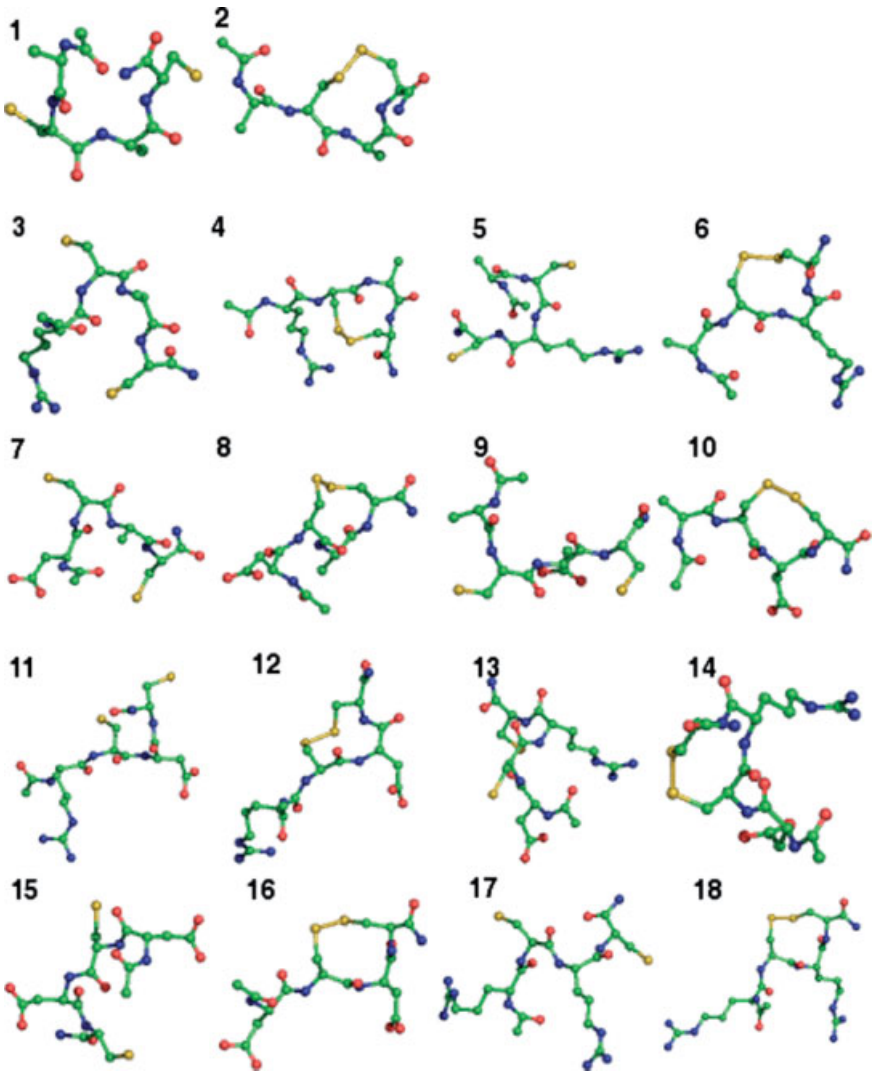

Figure 3 Ball and stick representation of the last frame (at 2.2 ns) from each molecular dynamics trajectory of the Ac-XCYC-NH_2 series. See Table 1 for sequence details of each analog. Hydrogen atoms are not rendered for the clarity of representation.

DOI: 10.1002/psc

both cases, almost the same states were observed with very similar average values of pdo_β. For example, the -A^2CR^4- residues in (*S*, *S*)Ac-A^2CRC^5-NH_2 are in the ACC state for 29.4% with average pdo_β value of $-93.8^\circ(\pm 39.4^\circ)$, resembling those in (*S*, *S*)Ac-A^2CAC^5-NH_2 with a population of 6.7% and an average value of pdo_β $-81.9^\circ(\pm 53.4^\circ)$ (Table 3). This fact indicates that alanine to arginine mutation had no strong impact on the backbone conformation. These results indicate that there is a strong dependence between a specific backbone conformation and the side-chain orientation.

Ac-D^2CAC^5-NH_2, (S,S)Ac-D^2CAC^5-NH_2. Compared to the previous cases, replacement of the *N*-terminal A^2 residue by D induced small changes on the distribution of pdo_β angle values in the linear Ac-D^2CAC^5-NH_2 (Figure 2). The adopted pdo_β values exhibited a well-centered peak at approximately $+120^\circ$. On the other hand the backbone conformation of the linear analog did not form any stable cluster (Table 3). In this case, upon cyclization a slight preference for an *antiplanar* rather than a *synplanar* orientation of the D^2 and A^4 side chains was observed (Figure 2).

Ac-A^2CDC^5-NH_2, (S,S)Ac-A^2CDC^5-NH_2. Contrary to the previous cases, these two analogs did not show a flat distribution of the pdo_β values. The pdo_β of Ac-A^2CDC^5-NH_2 and (*S*, *S*)Ac-A^2CDC^5-NH_2 have two peaks, each centered approximately at -60° and $+60^\circ$ and at $\sim 0^\circ$ and $+160^\circ$ respectively. The shift of the pdo_β distribution at $\sim 0^\circ$ indicates that cyclization clearly favors the *synplanar* orientation of the A^2 and D^4 side chains ($\sim$33%) (Figure 2, Table 2). However, in a high percentage of frames the corresponding side chains remain in the *antiplanar* orientation (Figure 2). Differences were also observed for the backbone conformational states of Ac-A^2CDC^5-NH_2 compared to the Ac-A^2CAC^5-NH_2 and the Ac-A^2CRC^5-NH_2 analogs. The backbone conformation of the -A^2CD^4-fragment was found to form several clusters having, however, as common element the A conformational state of the aspartic residue. Upon cyclization this residue adopts the C state in all clusters.

Ac-R^2CDC^5-NH_2, (S,S)Ac-R^2CDC^5-NH_2. In these two analogs the ionic interaction could be established. As is seen in Figure 2 the synergic effect of both factors (ionic interaction and cyclization) leads to a relatively narrow distribution of the *pdo* and pdo_β values. In the linear compound the values of pdo_β are distributed with a maximum at approximately $+140^\circ$ (Figure 2). This fact indicates that the ionic interaction itself cannot induce a *synplanar* orientation of the R^2 and D^4 side chains. A measure of the effect of the ionic interaction on the orientation of the charged centers is the *pdo* values which are distributed with a maximum shifted at approximately $+75^\circ$. Disulfide cyclization induced an almost complete synplanar orientation of the R^2 and D^4 side chains with both the pdo_β and *pdo* values distributed with a maximum at approximately $+15^\circ$ (Figure 2). Unlike other linear analogs, Ac-R^2CDC^5-NH_2 had a relatively stable backbone conformation, which was reflected by a very populated cluster in the -R^2CD^4- fragment. The R^2 and D^5 residues have shown substantially reduced mobility during MD trajectory, and they were found mainly in the E and A states respectively (Table 3). Disulfide cyclization, like in the other cases, shifted the preference of the D^4 residue (between the two cysteines) from A to C conformational state. It is notable that all conformational clusters in (*S*, *S*)Ac-R^2CDC^5-NH_2 have both *pdo* and pdo_β average values within the $[-45^\circ, +45^\circ]$ region with low standard deviations ($<25^\circ$). The populations of the frames with *pdo* and pdo_β within the region $[-45^\circ, 45^\circ]$ are 75 and 80% respectively. The strong effect of the cyclization on the *synplanar* orientation of the charged side chains is clearly evidenced if we consider that the percentages for the *synplanar* and *antiplanar* orientations from $\sim$0 and $\sim$41% in the linear analog become $\sim$80 and $\sim$4% respectively in the cyclic compound.

Ac-D^2CRC^5-NH_2, (S,S)Ac-D^2CRC^5-NH_2. In this case, the distribution of the *pdo* and pdo_β values exhibited narrow and strong peaks, similar to those found for the Ac-R^2CDC^5-NH_2 and (*S*, *S*)Ac-R^2CDC^5-NH_2 analogs. However they were shifted to different regions. Thus, the *pdo* and pdo_β distribution peaks of Ac-D^2CRC^5-NH_2 were found at approximately -45° and -135° respectively. The corresponding values for (S,S)Ac-D^2CRC^5-NH_2 were -60° and -100° (Figure 2). Although the change in the pdo_β distribution upon cyclization indicated a tendency of inducing the *synplanar* orientation of the D^2 and R^4 side chains, the percentage of the frames with pdo_β within the region $[-45^\circ, 45^\circ]$ was found to be only 7% (Table 2). This value is considerably lower than that observed for the cyclic (S,S)Ac-R^2CDC^5-NH_2 ($\sim$80%). This fact indicates that the –RCD- sequence favors more efficiently a *synplanar* orientation of the arginine and aspartic acid side chains, than the -DCR- one. In the linear analog the preferred backbone conformational states for all four residues are in the A and B states. The residue between the two cysteines, as in the case of the other linear analogs, adopts the A conformational state and disulfide cyclization turns this preference for the C state.

Ac-R^2CRC^5-NH_2, (S,S)Ac-R^2CRC^5-NH_2, Ac-D^2CDC^5-NH_2, (S,S)Ac-D^2CDC^5-NH_2. The presence of two residues of the same charged side chain within the peptide sequence had revealed some differences in backbone conformation while pdo_β distribution was only slightly affected, compared to the sequences where only one charged side chain existed. For example Ac-R^2CRC^5-NH_2 showed very similar

DOI: 10.1002/psc

pdo_β distribution to the analogs Ac-R^2CAC^5-NH_2 and Ac-A^2CRC^5-NH_2 (Table 2, Figure 2). Disulfide cyclization of the Ac-R^2CRC^5-NH_2 analog also showed similar conformational preferences as in Ac-A^2CRC^5-NH_2 and Ac-A^2CRC^5-NH_2 cases. So, the percentage of pdo_β within [−45°, 45°] increased after cyclization from 0.3 to 9.7% while the percentage within [135°, −135°] decreased form 63.7 to 50.8%. Despite the similarities in pdo_β distribution, backbone conformation preferences were quite different. So conformational clusters observed in the (*S*, *S*)Ac-R^2CRC^5-NH_2 analog have not been observed in the analogs (*S*, *S*)Ac-R^2CAC^5-NH_2, (*S*, *S*)Ac-A^2CRC^5-NH_2 and (*S*, *S*)Ac-R^2CRC^5-NH_2 (Table 3). The (*S*, *S*)Ac-D^2CDC^5-NH_2 analog revealed very similar properties to the (*S*, *S*)Ac-A^2CAC^5-NH_2 analog concerning the pdo_β distribution (Figure 2) where a peak at approximately +15° was observed with 42.6% of the frames in *synplanar* orientation (Table 2). As in the (*S*, *S*)Ac-R^2CRC^5-NH_2 case, conformational clusters observed in the (*S*, *S*)Ac-A^2CDC^5-NH_2 and (*S*, *S*)Ac-D^2CAC^5-NH_2 analogs have not been observed in (*S*, *S*)Ac-D^2CDC^5-NH_2 and *vise versa* (Table 3). This fact indicates that peptide structures permit similar side-chain orientation through different backbone conformations.

The Ac-C^2XCY^5-NH_2 Class of Analogs

Ac-C^2ACA^5-NH_2, (S,S)Ac-C^2ACA^5-NH_2. These two analogs have similar pdo_β distributions, with a wide peak at approximately +135° (Figure 4). Unlike the Ac-A^2CAC^5-NH_2 and (*S*, *S*)Ac-A^2CAC^5-NH_2 analogs, in this case upon cyclization the percentage with *antiplanar* orientation of the alanines' side chains increases from ∼46 to ∼72% (Table 2). Contrary to the previous class of analogs (Ac-XCYC-NH_2), the alanine residue between the two cysteines remains in A or B conformational state and does not show any preference for the C conformational state after cyclization (Table 3). The pdo_β values found in the range [−45°, 45°] were less than 5% of the frames in both linear and cyclic analogs (Table 2). Ball and stick representations of the structures are shown in Figure 5.

Ac-C^2RCA^5-NH_2, (S,S)Ac-C^2RCA^5-NH_2 Ac-C^2DCA^5-NH_2, (S,S)Ac-C^2DCA^5-NH_2, Ac-C^2ACR^5-NH_2, (S,S)Ac-C^2ACR^5-NH_2, Ac-C^2DCR^5-NH_2, (S,S)Ac-C^2DCR^5-NH_2. As is shown in Figure 4 and Table 2, any replacement of A^3 and/or A^5 with R or D did not significantly modify the profile of the pdo_β distribution in either the linear or the cyclic analogs. In all cases, cyclization seems to induce a better stabilization of the *antiplanar* orientation of the X^3 and Y^5 side chains. This is clearly evidenced by the increased percentage, in all cases, of the frames having pdo_β values within the region of [135°, −135°] (Table 2). Interestingly, even the presence of the charged amino acids (the case of Ac-C^2DCR^5-NH_2) did not induce in any appreciable percentage the *synplanar* orientation of the arginine and aspartic acid side chains.

Ac-C^2RCD^5-NH_2, (S,S)Ac-C^2RCD^5-NH_2. Contrary to all the above cases, the analysis of the pdo_β distribution for the Ac-C^2RCD^5-NH_2 analog showed a sharp peak at −60° and a smaller one (and significantly wider) at +60° (Figure 4). Considering the backbone conformation of all four residues there was not observed any stable cluster (Table 3). Thus, the ionic interaction seems to restrict the pdo_β distribution, but does not stabilize the backbone conformation. This situation is quite different from that observed for the Ac-R^2CDC^5-NH_2 analog which adopted a very stable cluster. Cyclization of Ac-C^2RCD^5-NH_2 shifts the pdo_β values closer to 0° inducing a *synplanar* orientation of the R^3 and D^5 side chains. Approximately 57% of the pdo_β values were found within the range of [−45°, 45°]. Although this value is considerably lower than that observed in the case of the cyclic (*S*, *S*)Ac-R^2CD^4C-NH_2 (∼80%) the synergic effect of both, the disulfide cyclization and the ionic interaction, on the orientation of the charged side chains is well supported. On the other hand, the presence of four clusters for the cyclic analog (*S*, *S*)Ac-C^2RCD^5-NH_2 indicates a strong influence of the disulfide cyclization on the backbone conformation. The most populated cluster was found in the CEF state with 26.8% of frames (Table 3). Taking into account all the above presented results, we can conclude that, in the case of the linear and cyclic Ac-CXCY-NH_2 class of analogs, the *antiplanar* orientation of the X and Y side chains is favored. The single exception constitutes the Ac-CRCD-NH_2 and (*S*,*S*)Ac-CRCD-NH_2 analogs confirming that the -RCD- sequence favors more efficiently a *synplanar* orientation of the arginine and aspartic acid side chains, than the -DCR- one.

Ac-C^2RCR^5-NH_2, (S,S)Ac-C^2DCD^5-NH_2, Ac-C^2DCD^5-NH_2, (S,S)Ac-C^2DCD^5-NH_2. Replacement of A^3 and A^5 residues with either R- or D-residues did not significantly change the side-chain orientation observed in the analogs with only one charged residue. For example, the linear Ac-C^2DCD^5-NH_2 analog has shown very similar pdo_β distribution to Ac-C^2DCA^5-NH_2 (Figure 4). In the same manner, the cyclic (*S*, *S*)Ac-C^2DCD^5-NH_2 and (*S*, *S*)Ac-C^2DCA^5-NH_2 analogs showed quite similar pdo_β distributions, although in the case of the (*S*, *S*)Ac-C^2DCD^5-NH_2 analog *synplanar* side-chain orientation was found in 18.1% of the frames (Table 2) while this percentage in the (*S*, *S*)Ac-C^2DCA^5-NH_2 analog was only 0.1%. Very similarly, double A to R replacement revealed only minor differences in pdo_β distribution in the liner analog. Cyclic (*S*, *S*)Ac-C^2RCR^5-NH_2 analogue showed a remarkably high preference to *antiplanar* orientation of side chains, which was also observed in other cyclic analogs of the -CXCY-motif. This analog showed minimal percentage of pdo_β within [−45°, 45°] of only 1.0% while the

DOI: 10.1002/psc

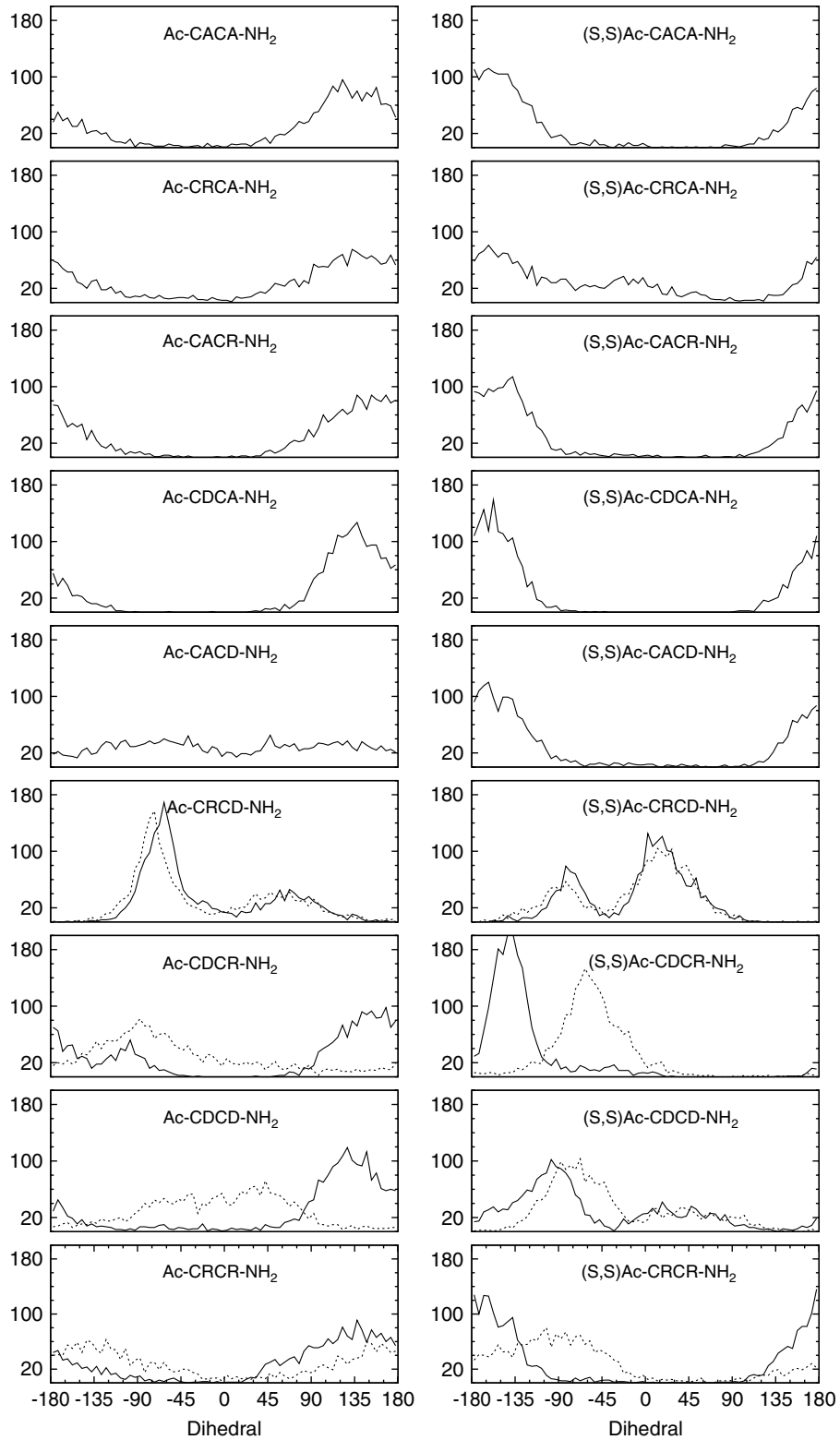

Figure 4 Vertical axis shows number of frames. pdo_β (lines) and *pdo* (dashed lines) distribution of the linear and cyclic analogs in the Ac-CXCY-NH_2 series.

corresponding percentage in the region [135°, −135°] was found to be 80.0%. Strong preference to *antiplanar* orientation of side chains was also observed in other analogs of the -CXCY- motif; for example in the (*S*, *S*)Ac-C^2ACA^5-NH_2 and (*S*, *S*)Ac-C^2DCA^5-NH_2 analogs, with percentages of *antiplanar* orientation 72.1% and 83.4%, respectively (Table 2). This fact indicates that the *antiplanar* preference is imposed by the -CXCY- motif and that the charge–charge repulsion does not have any particular impact on this preference.

DOI: 10.1002/psc

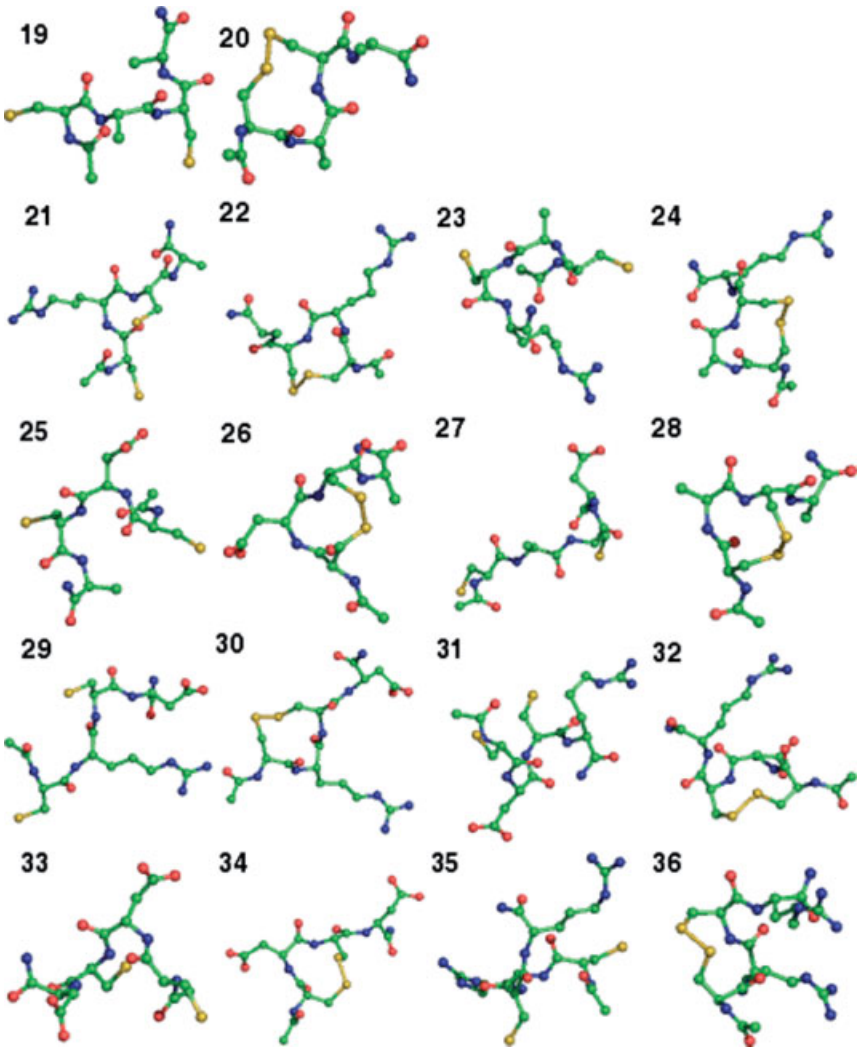

Figure 5 Ball and stick representation of the last frame (at 2.2 ns) from each molecular dynamics trajectory of the Ac-CXCY-NH_2 series. See Table 1 for sequence details of each analog. Hydrogen atoms are not rendered for the clarity of representation.

Comparison of Backbone Conformation with Other Disulfide Cyclic Peptides

A similar disulfide motif with very interesting structural implications is the -CXYC- motif, which has been found in many helical sequences [7]. The sequence -CAAC- has been also used for α-helix stabilization when placed at the N-terminal of designed peptides [7]. A direct comparison between -CXYC- and -XCYC- or -CXCY- motifs might not be appropriate, since in our motif one residue lies outside of the cyclic part of the peptide. It has been reported that -CXYC- motif has a turn structure and initiates a helical conformation. We did not observe a turn conformation in our study. Moreover, we do not provide any evidence for secondary structure propagation in peptides with bigger sequences, since our current study has been focused on shorter peptides. Future development will include this feature.

A very interesting example of experimentally determined structure of a peptide with the (*S*,*S*)-CXC- motif is that of the JOM-13 peptide [12–15]. This peptide has been found to bind the δ -opioid receptor. Its sequence is Tyr-c[D-Cys-Phe-D-Pen]OH and it has significant homology with compounds presented here. Some discrepancies anyway occur, such as the absence of capping groups, the Pen residue in the place of one Cys residue and the existence of two D-residues. Despite these differences, it is the analog with the greatest homology to our analogs. The structure of this compound has been determined both with molecular modeling and NMR techniques. The similarity of the structures was remarkable, especially in the cyclic part of the peptide. These findings support the validity of our proposed structures of the (*S*,*S*)-CXC analogs presented here. The presence of two D-residues greatly affected the peptide's structure and so a number of conformational dissimilarities have been observed. For example, while backbone φ dihedral angle of L-Phe residue (which stands between the Cys and Pen residues) was found to be -85° (we observed similar values in residues at the same position) the ψ backbone angle was found to vary in the range [-40°, -15°]. Overall this corresponds to

DOI: 10.1002/psc

the A conformational state, while our results indicate that in the majority of cases, the corresponding residue was found in the C conformational state. On the other hand, the pdo_{β} dihedral angle (which corresponds to the side chains of Tyr and Phe) was found to be 168°, thus in antiplanar conformation. While such values have also been observed in our study, this conformation was not the dominant one. Direct comparisons however should be carefully made and take into consideration the different nature and the chirality of the residues. As with the -CXYC- motif discussed previously, direct comparison of the -CXYC- structure with the structures presented here, to our opinion, might not be appropriate and relevant implementations should be made with care taking into consideration the impact of the D-/L-chirality of amino acid residues. However, future development of the current work can include D-residues in order to draw relevant conclusions about the influence of chirality on the cyclic structure and its consequences on the side-chain orientation. For example, similar computational studies, taking also into consideration D-/L-replacements, have been shown to be very useful on designing peptides as serine protease mimics [31–33].

CONCLUSIONS

In this work, we attempted to evaluate the influence of factors such as cyclization, charge–charge interactions, and sequence on the relative orientation of the side chains of the X and Y amino acids in the series of the linear and cyclic Ac-XCYC-NH_2 and Ac-CXCY-NH_2 peptide analogs. Thirty-six compounds were studied with classical MD. From the present study, it is concluded that in the linear compounds of both series the antiplanar orientation of the X and Y side chains is favored. Cyclization has a great impact on the *synplanar* orientation of the X and Y side chains in the (*S*,*S*)Ac-XCYC-NH_2 series of compounds. On the contrary, the *antiplanar* orientation is favored in the case of the (*S*,*S*)Ac-CXCY-NH_2 series, with a single exception in that of (*S*,*S*)Ac-CRCD-NH_2. Charge–charge interaction reduces the available conformational space of the side chains, but it has only a weak synergic effect on inducing a *synplanar* orientation of arginine and aspartic acid side chains. In addition to cyclization and ionic interaction, the sequence also contributes to the relative orientation of the X and Y side chains. Finally, it is concluded that the -CXC- motif can be used for inducing either a *synplanar* or an *antiplanar* orientation of side chains by choosing the *N*- or *C*-terminus peptide elongation respectively.

Acknowledgements

This research was co-funded by the European Union – European Social Fund (ESF) and National Sources, in the framework of the program 'Pythagoras II' of the 'Operational Program for Education and Initial Vocational Training' of the 3rd Community Support Framework of the Hellenic Ministry of Education.

REFERENCES

1. Gentilucci L, Tolomelli A, Squassabia F. Peptides and peptidomimetics in medicine, surgery and biotechnology. *Curr. Med. Chem.* 2006; **13**: 2449–2466.
2. Kee KS, Jois SD. Design of beta-turn based therapeutic agents. *Curr. Pharm. Des.* 2003; **9**: 1209–1224.
3. Lambert JN, Mitchell JP, Roberts KD. The synthesis of cyclic peptides. *J. Chem. Soc., Perkin Trans. 1* 2001:; 471–484.
4. Gupta A, Van Vlijmen HW, Singh J. A classification of disulfide patterns and its relationship to protein structure and function. *Protein Sci.* 2004; **13**: 2045–2058.
5. Jai Kartik V, Lavanya T, Guruprasad K. Analysis of disulphide bond connectivity patterns in protein tertiary structure. *Int. J. Biol. Macromol.* 2006; **38**: 174–179.
6. Chivers PT, Prehoda KE, Raines RT. The CXXC motif: a rheostat in the active site. *Biochemistry* 1997; **36**: 4061–4066.
7. Iqbalsyah TM, Moutevelis E, Warwicker J, Errington N, Doig AJ. The CXXC motif at the N terminus of an alpha-helical peptide. *Protein Sci.* 2006; **15**: 1945–1950.
8. Kallblad P, Dean PM. Efficient conformational sampling of local side-chain flexibility. *J. Mol. Biol.* 2003; **326**: 1651–1665.
9. Bower MJ, Cohen FE, Dunbrack RL Jr. Prediction of protein side-chain rotamers from a backbone-dependent rotamer library: a new homology modeling tool. *J. Mol. Biol.* 1997; **267**: 1268–1282.
10. Dunbrack RL Jr. Rotamer libraries in the 21st century. *Curr. Opin. Struct. Biol.* 2002; **12**: 431–440.
11. Ogata K, Umeyama H. Prediction of protein side-chain conformations by principal component analysis for fixed main-chain atoms. *Protein Eng.* 1997; **10**: 353–359.
12. Mosberg HI, Lomize AL, Wang C, Kroona H, Heyl DL, Sobczyk-Kojiro K, Ma W, Mousigian C, Porreca F. Development of a model for the delta opioid receptor pharmacophore. 1. Conformationally restricted Tyr1 replacements in the cyclic delta receptor selective tetrapeptide Tyr-c[D-Cys-Phe-D-Pen]OH (JOM-13). *J. Med. Chem.* 1994; **37**: 4371–4383.
13. Mosberg HI, Omnaas JR, Lomize A, Heyl DL, Nordan I, Mousigian C, Davis P, Porreca F. Development of a model for the delta opioid receptor pharmacophore. 2. Conformationally restricted Phe3 replacements in the cyclic delta receptor selective tetrapeptide Tyr-c[D-Cys-Phe-D-Pen]OH (JOM-13). *J. Med. Chem.* 1994; **37**: 4384–4391.
14. Lomize AL, Pogozheva ID, Mosberg HI. Development of a model for the delta-opioid receptor pharmacophore: 3. Comparison of the cyclic tetrapeptide, Tyr-c[D-Cys-Phe-D-Pen]OH with other conformationally constrained delta-receptor selective ligands. *Biopolymers* 1996; **38**: 221–234.
15. Mosberg HI, Dua RK, Pogozheva ID, Lomize AL. Development of a model for the delta-opioid receptor pharmacophore. 4. Residue 3 dehydrophenylalanine analogues of Tyr-c[D-Cys-Phe-D-Pen]OH (JOM-13) confirm required gauche orientation of aromatic side chain. *Biopolymers* 1996; **39**: 287–296.
16. Stavrakoudis A, Bizos G, Eleftheriadis D, Kouki A, Panou-Pomonis E, Sakarellos-Daitsiotis M, Sakarellos C, Tsoukatos D, Tsikaris V. A three-residue cyclic scaffold of non-RGD containing peptide analogues as platelet aggregation inhibitors: design, synthesis, and structure–function relationships. *Biopolymers* 2000–2001; **56**: 20–26.
17. Kouki A, Mitsios JV, Sakarellos-Daitsiotis M, Sakarellos C, Tselepis AD, Tsikaris V, Tsoukatos DC. Highly constrained cyclic (S,S) -CXaaC- peptides as inhibitors of fibrinogen binding to platelets. *J. Thromb. Haemostasis* 2005; **3**: 2324–2330.

18. Stote RH. Analysis of the RGD sequence in protein structures: comparison to the conformations of the RGDW and DRGDW peptides determined by molecular dynamics simulations. *Theor. Chem. Acc.* 2001; **2001**: 128–136.
19. Kostidis S, Stavrakoudis A, Biris N, Tsoukatos D, Sakarellos C, Tsikaris V. The relative orientation of the Arg and Asp side chains defined by a pseudodihedral angle as a key criterion for evaluating the structure-activity relationship of RGD peptides. *J. Pept. Sci.* 2004; **10**: 494–509.
20. Hansson T, Oostenbrink C, van Gunsteren WF. Molecular dynamics simulations. *Curr. Opin. Struct. Biol.* 2002; **12**: 190–196.
21. Karplus M, McCammon JA. Molecular Dynamics simulations of biomolecules. *Nat. Struct. Biol.* 2002; **9**: 646–652.
22. Ponder JWW, Richards FM. An efficient newton-like method for molecular mechanics energy minimization of large molecules. *J. Comput. Chem.* 1987; **8**: 1016–1024.
23. Ponder JW, Case DA. Force fields for protein simulations. *Adv. Protein Chem.* 2003; **66**: 27–85.
24. Ooi T, Oobatake M, Nemethy G, Scheraga HA. Accessible surface areas as a measure of the thermodynamic parameters of hydration of peptides. *Proc. Natl. Acad. Sci. U.S.A.* 1987; **84**: 3086–3090.
25. Feig M, Brooks CL 3rd. Recent advances in the development and application of implicit solvent models in biomolecule simulations. *Curr. Opin. Struct. Biol.* 2004; **14**: 217–224.
26. Im W, Chen J, Brooks CL 3rd. Peptide and protein folding and conformational equilibria: theoretical treatment of electrostatics and hydrogen bonding with implicit solvent models. *Adv. Protein Chem.* 2005; **72**: 173–198.
27. Humphrey W, Dalke A, Schulten K. VMD: visual molecular dynamics. *J. Mol. Graphics* 1996; **14**: 33–38.
28. Koradi R, Billeter M, Wuthrich K. MOLMOL: a program for display and analysis of macromolecular structures. *J. Mol. Graphics* 1996; **14**: 51–55.
29. Zimmerman SS, Pottle MS, Nemethy G, Scheraga HA. Conformational analysis of the 20 naturally occurring amino acid residues using ECEPP. *Macromolecules* 1977; **10**: 1–9.
30. Frishman D, Argos P. Knowledge-based protein secondary structure assignment. *Proteins* 1995; **23**: 566–579.
31. Stavrakoudis A, Makropoulou S, Tsikaris V, Sakarellos-Daitsiotis M, Sakarellos C, Demetropoulos IN. Computational screening of branched cyclic peptide motifs as potential enzyme mimetics. *J. Pept. Sci.* 2003; **9**: 145–155.
32. Tatsis V, Stavrakoudis A, Demetropoulos IN. LysinebasedTrypsin-ActSite(LysTAS): a configurational tool of the TINKER software to evaluate Lysine based branched cyclic peptides as potential chymotrypsin-mimetics. *Mol. Simul.* 2006; **32**: 643–644.
33. Tatsis VA, Stavrakoudis A, Demetropoulos IN. Molecular Dynamics as a pattern recognition tool: an automated process detects peptides that preserve the 3D arrangement of Trypsin's Active Site. *Biophys. Chem.* 2008; **133**: 36–44.

DOI: 10.1002/psc